GBAS use cases beyond what was envisioned – drone navigation

Sophie Jochems, Michael Felux, Philipp Schnüriger, *Zurich University of Applied Sciences, Center for Aviation*
Michael Jäger, Luciano Sarperi, *Zurich University of Applied Sciences, Institute of Signal Processing and Wireless Communications*

ABSTRACT

In this paper, we investigate the potential performance of the envisioned Differentially Corrected Positioning Service (DCPS) for the Ground Based Augmentation System (GBAS). For this purpose, we receive and decode the GBAS messages transmitted by the operational GBAS station providing GBAS Approach Service Type (GAST) C (i.e. a CAT-I service) at Zurich airport. Based on these parameters we calculate the respective protection levels for the GBAS DCPS and compare them with the SBAS protection levels. Due to the fact, that the GBAS corrections are locally generated, the achievable performance is usually better than with SBAS. However, the GNSS navigation errors decorrelate with distance, leading to an increase in the protection level. Both, the GBAS and SBAS protection levels, are dependent on a k-factor. This factor is derived from the allocated integrity risk to an integrity risk and equals 6.18 in the case of SBAS. For GBAS, the k-factor is 10. This is a very conservative value, which would be adapted in the future as the DCPS, its use-cases and the required level of integrity are developed further. To show a less conservative and more realistic scenario for comparing SBAS and GBAS protection levels, a GBAS protection level with a reduced k-factor of 6.18 was additionally calculated. The resulting performance of the regular GBAS and the GBAS with a reduced k-factor is then compared to the protection levels of a purely SBAS-based navigation to identify areas of potential use of the proposed system. Based on these evaluations we show that the GBAS DCPS yields better performance in an area of (on average) more than 50 km around the GBAS station.

INTRODUCTION

The Ground Based Augmentation System (GBAS) is a precision approach and landing system which provides corrections for GPS navigation signals and integrity parameters to airborne users. Those parameters are transmitted via a VHF data broadcast. The broadcast is freely accessible and can therefore be received and decoded by virtually everyone. A GBAS ground station is located within the security perimeter of an airport, uses high-quality equipment that allows to keep errors to a minimum and furthermore, provides guaranteed levels of performance by specification and continuously self-monitors the integrity of the information provided. The currently provided GBAS approach service, by design, only serves a very specific purpose: aircraft equipped with the appropriate avionics can use the provided information to correct GPS signals and ensure that all integrity requirements are met. Moreover they can use the information regarding the approach geometry in the GBAS message to output deviations from the reference approach trajectory to the (auto-)pilot and provide precision approach guidance. The actual differentially corrected position is currently not used. A differentially corrected position service (DCPS) type is envisioned and standardized, but currently no operational stations provide this service.

GBAS to date is not very widely used because i) not many airports are equipped with a GBAS ground station and ii) depending on the airport, not much of the fleet operating in and out is equipped with the GBAS landing system (GLS). The reason for this is a classic chicken/egg problem: On the one hand, the Air Navigation Service Provider (ANSP), or in some cases also the airport operator, is responsible for the installation, operation, and maintenance of a GBAS ground station. As this requires substantial investments and recurring costs (e.g. for flight inspection), not many ANSPs and/or airports are willing or are even able to install such a ground station without a solid business case. Especially because often only a few aircraft operating at this airport are suitably equipped to fly a GLS approach, it is currently still very difficult to generate operational benefits from a GBAS, such as increased throughput in low-visibility conditions or reduced critical and sensitive areas protecting the Instrument Landing System (ILS) signals. On the other hand, there are the aircraft operators. For them, it is also financially not very rewarding to equip their aircraft with the required receiver as there may be only a few destinations within their network where flying a GLS approach is actually possible and might bring operational benefits.

 https://doi.org/10.33012/2022.18213

Against this background, this paper discusses whether GBAS can provide benefits in another context, to more users and for different services. Additional use-cases might support the business case for GBAS on the one hand and provide other users with a solution to their unique challenges on the other hand. The potential use-case evaluated in this paper is the emerging field of UAV navigation. More specifically, a comparison between the performance of freely and readily available Satellite-Based Augmentation System (SBAS) and GBAS augmented positioning is presented. The concept explored in this work is to simulate GBAS positioning service protection level using integrity parameters transmitted by the operational GBAS at Zurich airport, and compare them to SBAS (EGNOS) protection levels. The aim is to show the potential benefit of GBAS in comparison with SBAS, and more specifically, the respective protection levels. In future work, it is envisioned to receive corrections provided by a GBAS ground station, forward them to a drone via data link or the cell phone network and re-use the information for drone guidance. In that way, existing corrections and integrity parameters could be re-used in a meaningful way without significant effort or changes to any existing system.

THEORY

For navigation systems used in aviation, two important performance indicators are highly relevant. The first one is the accuracy of the system, i.e. by how much the estimated position differs from the true position. The second important factor is the associated integrity, i.e. the measure of trust that can be placed in the correctness of the estimated position. Integrity is usually expressed by a so-called protection level (PL) associated with a pre-defined integrity risk. The protection level is an upper bound on the actual position error and is only exceeded with a probability of less than the specified integrity risk.
To improve accuracy of GNSS-based navigation, satellite-based and ground-based augmentation systems provide corrections for GNSS pseudo-range measurements that allow airborne users to correct their own GNSS pseudo-range measurement and eliminate large portions of the GNSS standalone errors. In addition, those systems provide integrity parameters that allow users to calculate error bounds associated to the position estimate. Those protection levels are then compared to so-called alert limits, i.e. the largest value that the PL may take so that the operation is still considered to be safe.
The equations for calculation of the SBAS and GBAS protection levels are defined in ICAO Annex 10 Volume I [1] and reproduced for convenience. Since the envisioned GBAS service is the DCPS, only the horizontal protection levels for the GBAS positioning service are considered for the GBAS case. Note that for the DCPS no vertical protection levels are currently specified since in aviation (except for precision approach guidance), vertical information is obtained from barometric altimetry. In SBAS the PLs for the non-precision approach case are evaluated.

SBAS protection level
The SBAS horizontal protection level for non-precision approach (NPA) modes is calculated as

$$HPL_{SBAS} = K_{H,NPA} * d_{major} \tag{1}$$

with

$$d_{major} = \sqrt{\frac{d_x^2 + d_y^2}{2} + \sqrt{\left(\frac{d_x^2 - d_y^2}{2}\right)^2 + d_{xy}^2}} \tag{2}$$

and $K_{H,NPA} = 6.18$. In this equation, d_{major} describes the standard deviation of the uncertainty of the horizontal position error that results from the satellite geometry and the uncertainties in the individual pseudo-range measurements. The k-factor inflates that value according to the allocated integrity risk. In more detail, the three terms d_x^2, d_y^2 and d_{xy}^2 are defined as:

$$d_x^2 = \sum_{i=1}^{N} s_{x,i}^2 * \sigma_i^2 \tag{3}$$

$$d_y^2 = \sum_{i=1}^{N} s_{y,i}^2 * \sigma_i^2 \tag{4}$$

$$d_{xy}^2 = \sum_{i=1}^{N} s_{x,i}^2 * s_{y,i}^2 * \sigma_i^2 \tag{5}$$

where $s_{x,i}$ and $s_{y,i}$ "are the partial derivative of position error in the x- / y-direction respectively with respect to pseudo-range error on the i[th] satellite" [1]. The residual uncertainties associated with the pseudo-range measurement σ_i^2 in the SBAS-case are defined as

$$\sigma_i^2 = \sigma_{i,flt}^2 + \sigma_{i,UIRE}^2 + \sigma_{i,air}^2 + \sigma_{i,tropo}^2 \quad (6)$$

The more detailed individual descriptions of the variances can be found in the ICAO Annex 10 Volume I and a detailed description is omitted here for brevity. The projection matrix *S* and the weighting matrix *W* are defined as

$$S \equiv \begin{bmatrix} s_{x,1} & s_{x,2} & \cdots & s_{x,N} \\ s_{y,1} & s_{y,2} & \cdots & s_{y,N} \\ s_{v,1} & s_{v,2} & \cdots & s_{v,N} \\ s_{t,1} & s_{t,2} & \cdots & s_{t,N} \end{bmatrix} = (G^T \, x \, W \, x \, G)^{-1} \, x \, G^T \, x \, W \quad (7)$$

$$W = \begin{bmatrix} \sigma_1^2 & 0 & \cdots & 0 \\ 0 & \sigma_2^2 & \cdots & 0 \\ \vdots & \vdots & \ddots & \vdots \\ 0 & 0 & \cdots & \sigma_N^2 \end{bmatrix}^{-1} \quad (8)$$

where

$$G_i = [-cos\ El_i \ cos\ Az_i \ -cos\ El_i \ sin\ Az_i \ -sin\ El_i \ 1] \quad (9)$$

El_i is the elevation angle and Az_i the azimuth of the i[th] ranging source, respectively, the latter taken counter-clockwise from the x-axis [1].

GBAS protection level

The GBAS horizontal protection level (HPL_{GBAS}) for the positioning service is calculated in a similar way. In addition to the nominal protection level (HPL_{H0}) another protection level is calculated for a fault case (HPL_{H1}). Moreover, a horizontal ephemeris error position bound (HEB) is calculated. The HPL_{GBAS} corresponds to the largest of the three values HPL_{H0}, HPL_{H1} and HEB as shown in equation (10). The main calculation of HPL_{H0} can be seen in equations (11) and (12). The calculation of HPL_{H1} is described in equations (22) to (24) and the one of HEB in equation (30).

$$HPL_{GBAS} = MAX\{HPL_{H0}, HPL_{H1}, HEB\} \quad (10)$$

Nominal measurements conditions

The residual horizontal position error in the nominal case is bounded by

$$HPL_{H0} = K_{ffmd,POS} * d_{major} \quad (11)$$

with

$$d_{major} = \sqrt{\frac{d_x^2 + d_y^2}{2} + \sqrt{\left(\frac{d_x^2 - d_y^2}{2}\right)^2 + d_{xy}^2}} \quad (12)$$

where $K_{ffmd,POS} = 10$. Note that the factor of 10 is a very conservative choice that would be adapted in the future as the DCPS, its use-cases and the required level of integrity are developed further. The three terms d_x^2, d_y^2 and d_{xy}^2 are again defined as:

$$d_x^2 = \sum_{i=1}^{N} s_{x,i}^2 * \sigma_i^2 \quad (13)$$

$$d_y^2 = \sum_{i=1}^{N} s_{y,i}^2 * \sigma_i^2 \quad (14)$$

$$d_{xy}^2 = \sum_{i=1}^{N} s_{x,i}^2 * s_{y,i}^2 * \sigma_i^2 \quad (15)$$

where $s_{x,i}$ and $s_{y,i}$ are again the entries of the weighted pseudoinverse of the geometry matrix and the σ_i^2 are defined as

$$\sigma_i^2 = \sigma_{pr\_gnd,i}^2 + \sigma_{tropo,i}^2 + \sigma_{pr\_air,i}^2 + \sigma_{iono,i}^2 \quad (16)$$

The definitions of the variances describe the uncertainty attributed to the ground system ($\sigma_{pr\_gnd,i}^2$), the residual tropospheric uncertainty ($\sigma_{tropo,i}^2$), contribution of the airborne measurement uncertainty due to noise and multipath ($\sigma_{pr\_air,i}^2$) and the residual ionospheric uncertainty ($\sigma_{iono,i}^2$). These parameters are further discussed in the next section of the paper.

The projection matrix *S* and the weight matrix *W* are

$$S \equiv \begin{bmatrix} s_{x,1} & s_{x,2} & \cdots & s_{x,N} \\ s_{y,1} & s_{y,2} & \cdots & s_{y,N} \\ s_{v,1} & s_{v,2} & \cdots & s_{v,N} \\ s_{t,1} & s_{t,2} & \cdots & s_{t,N} \end{bmatrix} = (G^T \, x \, W \, x \, G)^{-1} \, x \, G^T \, x \, W \quad (17)$$

$$W = \begin{bmatrix} \sigma_{w,1}^2 & 0 & \cdots & 0 \\ 0 & \sigma_{w,2}^2 & \cdots & 0 \\ \vdots & \vdots & \ddots & \vdots \\ 0 & 0 & \cdots & \sigma_{w,N}^2 \end{bmatrix}^{-1} \quad (18)$$

where

$$G_i = [-cos\ El_i \ cos\ Az_i \ -cos\ El_i \ sin\ Az_i \ -sin\ El_i \ 1] \quad (19)$$

and

$$\sigma_{w,i}^2 = \sigma_{pr\_gnd,i}^2 + \sigma_{tropo,i}^2 + \sigma_{pr\_air,i}^2 + \sigma_{iono,i}^2 \quad (20)$$

With the same definitions as previously described in the SBAS case.

Faulted measurements conditions

In addition to the HPL_{H0}, another protection level is calculated for a single reference receiver fault given as

$$HPL_{H1} = max[HPL_j] \quad (21)$$

where HPL_j for j = 1 to 4 is

$$HPL_j = |B\_horz_j| + K_{md,POS} * d_{major,H1} \quad (22)$$

with $K_{md,POS} = 5.3$. B_horz_j and $d_{major,H1}$ are defined as following (equations (23) and (24)):

$$B\_horz_j = \sqrt{\left(\sum_{i=1}^{N} S_{x,i} * B_{i,j}\right)^2 + \left(\sum_{i=1}^{N} S_{y,i} * B_{i,j}\right)^2} \quad (23)$$

$$d_{major,H1} = \sqrt{\frac{d\_H1_x^2 + d\_H1_y^2}{2} + \sqrt{\left(\frac{d\_H1_x^2 - d\_H1_y^2}{2}\right)^2 + d\_H1_{xy}^2}} \quad (24)$$

where the $B_{i,j}$ are the "broadcast differences between the broadcast pseudo-range corrections and the corrections obtained excluding the j[th] reference receiver measurement for the i[th] ranging source" [1]. The B-values are broadcasted in the GBAS message and are indicating how well the 4 reference receivers are in agreement when determining the pseudo-range corrections. Larger B-values may indicate an issue with the respective reference receiver j. The three terms $d\_H1_x^2$, $d\_H1_y^2$ and d_H1_{xy} are defined as

$$d\_H1_x^2 = \sum_{i=1}^{N} s_{x,i}^2 * \sigma\_H1_i^2 \quad (25)$$

$$d\_H1_y^2 = \sum_{i=1}^{N} s_{y,i}^2 * \sigma\_H1_i^2 \quad (26)$$

$$d\_H1_{xy} = \sum_{i=1}^{N} s_{x,i} * s_{y,i} * \sigma\_H1_i^2 \quad (27)$$

where

$$\sigma\_H1_i^2 = \left(\frac{M_i}{U_i}\right) * \sigma_{pr\_gnd,i}^2 + \sigma_{pr\_air,i}^2 + \sigma_{tropo,i}^2 + \sigma_{iono,i}^2 \quad (28)$$

M_i is the "number of reference receivers used to compute the pseudo-range corrections for the i[th] ranging source (indicated by the B-value)" and U_i is the number of receivers used to determine pseudo-range i, excluding the receiver j [1].

Horizontal ephemeris error position bound

Finally, in order to account for the fact that GBAS is a local system and potential positioning errors due to ephemeris errors would increase with increasing distance from the GBAS ground station, a horizontal position error bound on the ephemeris error is calculated as

$$HEB_j = MAX\{HEB_j\} \quad (29)$$

$$HEB_j = \left|s_{horiz,j}\right| * x_{air} * P_j + K_{md\_e\_POS} * d_{major} \quad (30)$$

where

$$s_{horiz,j} = s_{xj}^2 + s_{yj}^2 \quad (31)$$

and x_{air} is the distance of the user from the GBAS reference point. The P_i is the ephemeris decorrelation parameter that is broadcasted by the ground station and describes how well the GBAS is able to monitor for potential ephemeris errors. For the calculation of d_{major} refer to equation (12) and the k-factor again inflates the error uncertainty according to the allocated integrity risk.

Comparison SBAS/GBAS

If we take a closer look at the calculations used for the HPL_{SBAS} and the HPL_{GBAS}, it becomes obvious that they are quite similar in nature. Table 1 contains a direct comparison of the most important equations used to calculate the SBAS and the GBAS protection level.

Table 1: Comparison of the SBAS and GBAS protection level calculation

SBAS protection level	**GBAS positioning service protection level**
$HPL_{SBAS} = K_{H,NPA} * d_{major}$ $K_{H,NPA} = 6.18$	$HPL_{H0} = K_{ffmd,POS} * d_{major}$ $K_{ffmd,POS} = 10$
$d_{major} = \sqrt{\frac{d_x^2 + d_y^2}{2} + \sqrt{\left(\frac{d_x^2 - d_y^2}{2}\right)^2 + d_{xy}^2}}$	$d_{major} = \sqrt{\frac{d_x^2 + d_y^2}{2} + \sqrt{\left(\frac{d_x^2 - d_y^2}{2}\right)^2 + d_{xy}^2}}$
$\sigma_i^2 = \sigma_{i,flt}^2 + \sigma_{i,UIRE}^2 + \sigma_{i,air}^2 + \sigma_{i,tropo}^2$	$\sigma_i^2 = \sigma_{pr\_gnd,i}^2 + \sigma_{tropo,i}^2 + \sigma_{pr\_air,i}^2 + \sigma_{iono,i}^2$
$S \equiv \begin{bmatrix} s_{x,1} & s_{x,2} & \cdots & s_{x,N} \\ s_{y,1} & s_{y,2} & \cdots & s_{y,N} \\ s_{v,1} & s_{v,2} & \cdots & s_{v,N} \\ s_{t,1} & s_{t,2} & \cdots & s_{t,N} \end{bmatrix}$ $= (G^T \, x \, W \, x \, G)^{-1} \, x \, G^T \, x \, W$	$S \equiv \begin{bmatrix} s_{x,1} & s_{x,2} & \cdots & s_{x,N} \\ s_{y,1} & s_{y,2} & \cdots & s_{y,N} \\ s_{v,1} & s_{v,2} & \cdots & s_{v,N} \\ s_{t,1} & s_{t,2} & \cdots & s_{t,N} \end{bmatrix}$ $= (G^T \, x \, W \, x \, G)^{-1} \, x \, G^T \, x \, W$
$W = \begin{bmatrix} \sigma_1^2 & 0 & \cdots & 0 \\ 0 & \sigma_2^2 & \cdots & 0 \\ \vdots & \vdots & \ddots & \vdots \\ 0 & 0 & \cdots & \sigma_N^2 \end{bmatrix}^{-1}$	$W = \begin{bmatrix} \sigma_{w,1}^2 & 0 & \cdots & 0 \\ 0 & \sigma_{w,2}^2 & \cdots & 0 \\ \vdots & \vdots & \ddots & \vdots \\ 0 & 0 & \cdots & \sigma_{w,N}^2 \end{bmatrix}^{-1}$

One significant difference is visible in the first row of the table. Whereas the k-factor for SBAS is 6.18, the corresponding value for GBAS equals 10. These values are multiplier derived from the probability of fault-free missed detection and correspond to the integrity risk. As already mentioned, the k-factor of 10 for GBAS is a very conservative value. d_{major} is calculated in exactly the same way for HPL_{SBAS} and HPL_{GBAS} with the only difference arising from the different σ_i^2 describing the respective uncertainties of the corrected pseudo-range measurements for the different systems in the appropriate ways. The *S* matrix is again the same in principle in both cases, with the only difference arising from the different weights resulting from the different uncertainties in the weighting matrices *W*.

METHODS

With the protection levels discussed, it is now possible to assess and compare the protection level performance for the different augmentation systems. In order to obtain the required parameters for a realistic assessment of the GBAS performance we implemented a GBAS receiver based on a software-defined radio stick to receive and decode the messages broadcasted by the GBAS at Zurich airport. In the implementation we followed the specifications from the Interface Control Document [2]. It is important to mention here that the GBAS in Zurich does not support the positioning service, it is only broadcasting corrections and the associated integrity parameters for the approach service. The results generated here are therefore purely experimental. However, the integrity parameters used for our evaluations would likely not change for the different services.
Specifically, the calculation of the individual uncertainties was carried out using the following parameters:

For $\sigma_{pr\_gnd,i}$: The broadcast values of the GBAS vary between 0.24 m and 0.4 m. Note that this may include inflations as part of the geometry screening process [3]. As a general tendency, the broadcast parameters are large for satellites just at or above 5 ° elevation but then decrease very quickly. In order to have a deterministic model for the behavior we decided to raise the elevation mask to 7 ° but then assume a constant value of 0.28 m for all satellites in our simulations. This is still a rather conservative value as the values are mostly 0.26 m.

For $\sigma_{pr\_air,i}$: According to [1],

$$\sigma_{pr\_air,i}^2 = \sqrt{\sigma_{noise}^2 + \sigma_{multipath}^2} \tag{32}$$

Following the results that researchers at KAIST derived with flight tests of their UAVs [4], we chose the standard multipath model

$$\sigma_{multipath}(el) = 0.13 + 0.53e^{-\frac{el}{10}} \quad (33)$$

Regarding the noise contribution of the receiver Boeing did a study using a Collins GLU-2100 state-of-the-art airborne receiver and determined that the receiver noise after smoothing was in the range of about 1 – 3 cm [5]. For the purpose of this study and due to the small contribution to the error we neglected the noise contribution. However, it should be noted that in UAV operations different receiver may be used.

The residual ionospheric uncertainty σ_{iono} is given as

$$\sigma_{iono} = F_{pp} \cdot \sigma_{vig} \cdot (x_{air} + 2\tau v_{air}) \quad (34)$$

The F_{pp} in the formula is a satellite elevation-dependent vertical-to-slant obliquity factor that accounts for the fact that the decorrelation of the ionospheric effect is described by σ_{vig}, the decorrelation for the vertical direction. The broadcast value is $\sigma_{vig} = 6.4 * 10^{-6}$. The term in parentheses describes the fact that the decorrelation increases with increasing distance x_{air} and speed v_{air}. For the use-case considered v_{air} is expected to be substantially smaller than the speeds that aircraft usually fly. For simulation purposes we are assuming a speed of 10 m/s. The parameter τ is the smoothing time constant, i.e. 100 s in the case considered in order to be in line with the smoothing time constant applied in the process of generating the GBAS corrections.

Finally, the residual tropospheric uncertainty σ_{tropo} is given by

$$\sigma_{tropo} = \sigma_n h_0 \frac{10^{-6}}{\sqrt{0.002+\sin^2(el)}}(1 - e^{-\Delta h/h_0}) \quad (35)$$

where σ_n is the refractivity uncertainty of the troposphere (broadcast value 13) and h_0 is the scale height of the troposphere (broadcast value 16 km). Both parameters are transmitted in Message Type 2 of the GBAS broadcast. The el in the denominator is the elevation of the satellite, and finally the parameter Δh is the height difference between the GBAS reference point and the user. For the use-case considered in the work, the height difference will be rather small as UAVs in many use-case scenarios stay at low altitudes to avoid potential conflicts with other airspace users. For this study we chose the height difference to be 100 m.

RESULTS

In this section we show the results obtained for SBAS protection levels and GBAS protection levels simulated with the previously described parameters.

For the evaluation of the horizontal SBAS protection level HPL_{SBAS}, data from our measurement station at the University of Applied Sciences in Winterthur, Switzerland was collected and evaluated with the Pegasus software tool from Eurocontrol [6]. Figure 1 shows the protection level over the course of one day (in this case the 17th of January 2022). On the x-axis, the time from 0 to 24 hours is displayed, the y-axis shows the horizontal protection level in meters. HPL_{SBAS} is only dependent on the satellite geometry, the SBAS parameters transmitted by the satellites (e.g. describing the state of the ionosphere) and local errors at the user side, i.e. mainly multipath. In general, the SBAS protection level tend to stay between 7 and 9 meters with occasional periods of time where they increase to about 11 to 14 m. After around 11 h, there is a significant peak with a HPL_{SBAS} of 51 m. This corresponds to a short drop to just 5 satellites used for about 4 seconds. Pegasus reports an SBAS message loss for that time period that likely occurred in our receiver. On average, the HPL_{SBAS} is about 8 m.

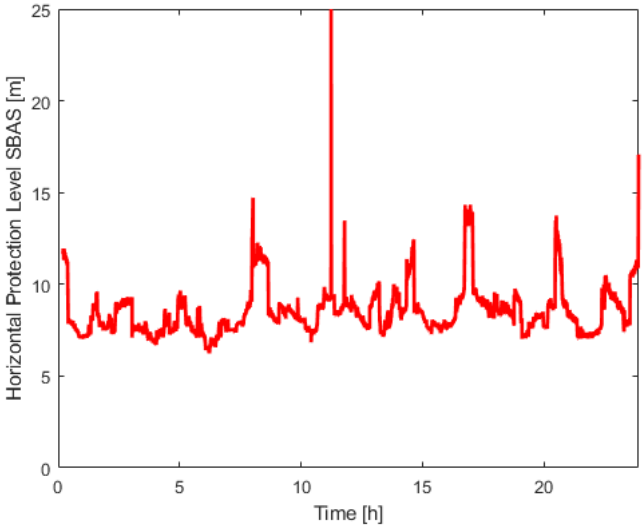

Figure 1: Development of HPL_{SBAS} over the course of 24 hours

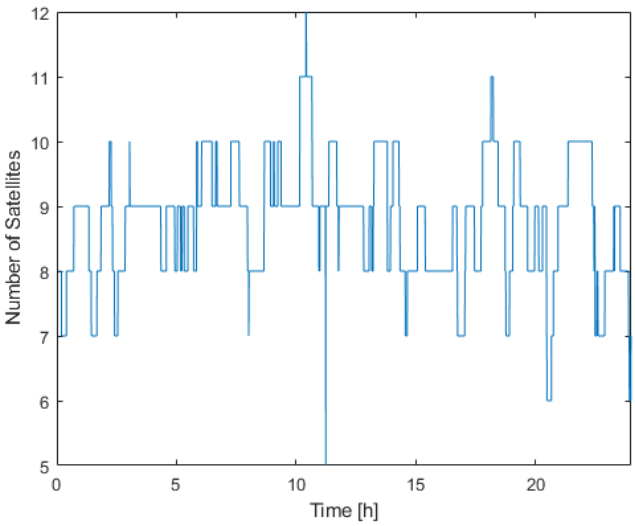

Figure 2: Number of satellites used over a course of 24 hours

The number of satellites used over the course of 24 hours is shown in Figure 2. It mostly varies between 8 and 10 with spikes up to 11 or 12 satellites. During few periods of time, the number of satellites used decreases to 7 or 6 and once to 5. These decreases to 8 or less satellites correspond to the peaks in the SBAS protection level. The already mentioned drop down to 5 satellites corresponding to the peak after 11 hours can be clearly seen. However, as already mentioned this was not due to geometry issues but due to exclusion in the processing for a message loss.

The SBAS scenario is used as the benchmark as it is freely available to all users and already implemented in a number of navigation systems for autonomous vehicles. The following part contrasts the SBAS performance with the obtainable performance when using the GBAS positioning service.

For HPL_{GBAS}, the protection level over the course of a day (24 hours) was calculated using the parameters detailed in the previous section. Figure 3 shows the results. On the x-axis, the time from 0 to 24 hours is displayed, the y-axis shows the horizontal protection level in meters. The colored lines represent the protection levels at different distances from the GBAS reference point. The HPL_{GBAS} assumes values between approximately 2 and 5 m (at a distance of just 1 km from the station) and lies between roughly 9 and 16 m (at 100 km from ZRH). The peak at around 17 h is the highest throughout the day and occurs for all distances due to the least favorable geometry and the drop in the number of visible satellites down to just 8.

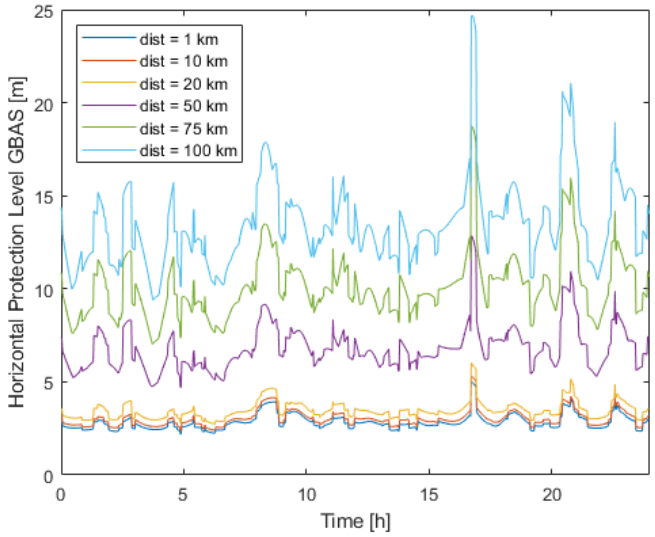

Figure 3: HPL_{GBAS} over the course of 24 hours

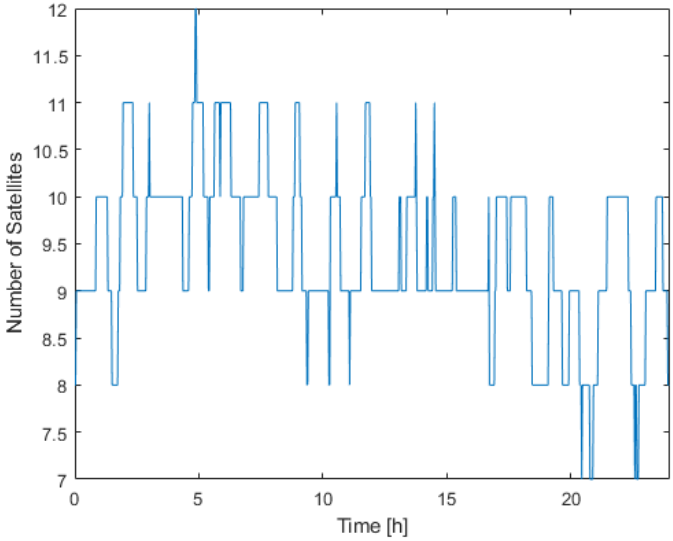

Figure 4: Number of available satellites over a course of 24 hours

The number of available satellites over the course of those 24 hours is illustrated in Figure 4. A minimum of 7 satellites was assumed to be available (all-in-view with a 7° elevation mask as described previously to account for the transmitted σ_{gnd}- values). The maximum occurs at around 5 h and corresponds to 12 satellites.

As seen in equation (10), HPL_{GBAS} is the maximum of three values, namely the nominal protection level HPL_{H0}, a fault-case protection level HPL_{H1} accounting for a single reference receiver fault in the GBAS ground station, and the horizontal error bound ephemeris *HEB*. In order to show the significance of the individual components of the final HPL, a more detailed analysis was performed. For this purpose, HPL_{H0}, HPL_{H1} and *HEB* were plotted for a fixed point in time (after roughly 21 hours) as a function of the distance to the GBAS station. Moreover, a HPL_{GBAS} with a reduced k-factor was calculated. The reason for this is the very conservative assumption of a k-factor of 10 for GBAS in comparison to a k-factor of 6.18 for SBAS, as discussed above. To illustrate potential improvements in performance by limiting the k-factor for GBAS to a smaller value, k was set to 6.18 for bounding to the same integrity risk as SBAS. In this way, the resulting protection level of GBAS and SBAS can be compared directly to each other. An example for such a plot with the regular HPL_{GBAS} (*HPL,pos regular*) and the newly calculated *HPL,pos reduced k* is illustrated in Figure 5. Besides *HPL,pos regular* (red background) and *HPL,pos reduced k* (green background), also *HPL,H0* (cyan, dotted line), *HPL,H0 reduced k* (cyan, plus-line), *HPL,H1* (magenta, dotted line) and *HEB,eph* (black, dotted line) are plotted. *HPL,H0 reduced k* is the protection level under nominal measurement conditions with a reduced k-factor of 6.18. All other variables are calculated regularly according to the previous equations.
The cyan dotted line with the red background shows the development of the *HPL,pos regular.* The fact, that the cyan dotted line is identical to *HPL,pos regular* means that *HPL,H0* is the dominant value up to a distance of roughly 18 km away from the GBAS station at this time. For a distance greater than 18 km, *HEB,eph* (black dotted line, green background) takes over and represents the dominant value. For *HPL,pos reduced k, HEB,eph* takes over very quickly from a distance greater than 5 km away from the ground station. It can be seen that *HPL,H1* does not play a role in this case, as it is never the dominant value for *HPL,pos regular*. This is to be expected, as the B-values transmitted by GBAS are usually very small. However, in the case of large, transmitted B-values indicating some disagreement between the reference receivers, the H1 protection level could increase significantly. Up to a distance of 18 km from the ground station, the horizontal protection level with a reduced k-factor is significantly lower than the protection level calculated with the regular k-factor. For distances greater than 18 km, the ephemeris error bound is the dominant value, thus there is no benefit anymore in the final protection level of the DCPS due to a reduced k-factor.
As mentioned above, the SBAS protection level has a mean value of around 8 m here in the Zurich area. From Figure 5, it can be seen that the *HEB,eph* stays below this value up to a distance of approximately 43 km away from the GBAS station in Zurich.

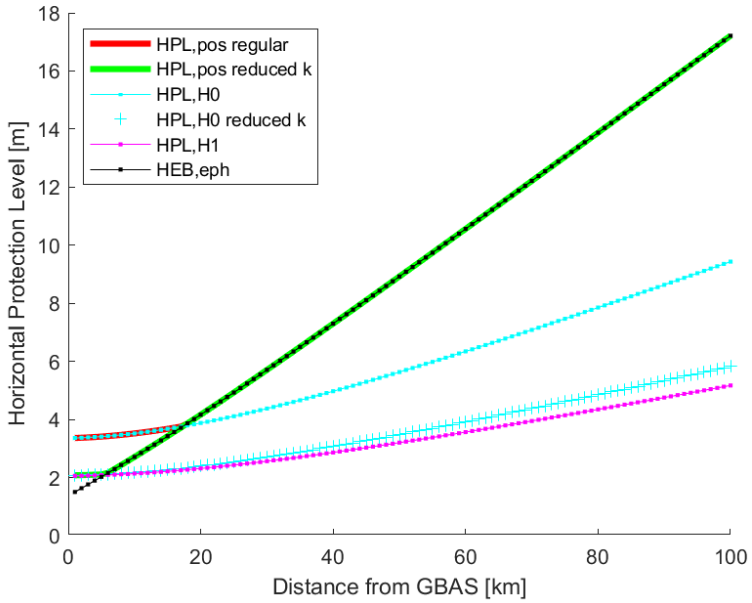

Figure 5: Different components of the positioning service protection level as a function of the distance from the GBAS station at ZRH

Since the protection levels are time dependent, the course of the above-described curves varies depending on the chosen point in time. Also, the distance from where *HEB,eph* takes over as the dominant value and up to which the protection level is lower than 8 m differs throughout the day. For this reason, we evaluated these two values throughout the day in steps of 1 h in time. *HEB,eph take-over* begins at between 18 and 36 km away from the GBAS ground station and *HPL,pos* becomes larger than 8 m between 29 and 80 km away from Zurich airport. On average, *HEB,eph* becomes dominant at a distance of about 25 km and *HPL,pos* is below the 8 m we chose as reference for the comparison to SBAS up to about 57 km.

DISCUSSION

In this work we only considered horizontal protection level behavior under nominal ionospheric conditions (i.e. the case that σ_{iono} is bounding the ionospheric errors). Other work previously done by Boeing and Stanford University [7,8,9] showed that an anomalous ionosphere can potentially create significant errors and needs to be considered and addressed. One possibility to ensure ionospheric conditions are nominal is the use of SBAS information where available, similar as it is already done in GBAS today. Another means would be to use GBAS corrections from multiple GBAS stations in a network-approach [10] to ensure any potential anomaly in the ionosphere would be detected. This approach is expected to work well in mid-latitudes as the ionosphere is well-behaved and anomalous ionospheric events are very rare.

In general, the GBAS PLs are smaller than the SBAS PLs up to an average distance of about 57 km to the GBAS station. This means that there is a significant potential benefit for UAV navigation applications in metropolitan areas where an airport is GBAS equipped. However, the area, where the use of GBAS instead of SBAS is beneficial, is limited. In the case of the GBAS station at Zurich airport, this area stretches roughly from Constance to Lucerne. While limited in size, these areas are probably the ones most likely for some significant amount of UAV applications and potential users.

The area in which a smaller HPL can be obtained by reducing the k-factor is somewhat smaller with an average distance of just about 25 km away from Zurich airport. The k-factor of 10 for HPL_{GBAS} seems unreasonably large, hence we suggest a reduction to e.g. 6.18 as for HPL_{SBAS}. With this reduced k, the area for potential performance improvements by smaller protection levels still includes the urban area of the cities of Zurich and Winterthur.

One other issue that can be observed by the results is the significant increase of the protection levels as soon as the number of satellites drops to 7 or less. The simulated results are all based on the all-in-view solution with a fixed elevation mask. However, especially when flying highly dynamic maneuvers with large attitude changes of the UAV, loss of tracking for satellites is likely. Hence, the operational performance is likely to be worse than the results shown here. However, it should be noted that the loss of satellites would equally affect GBAS DCPS and SBAS performance by weakening the geometry of the core constellation(s).

Finally, all these evaluations are just considering the use of the GPS constellation and the signals on the L1 frequency as these are the only navigation signals for which GBAS is currently providing corrections and integrity parameters. However, in the UAV-market many GNSS receiver chipsets already make use of multiple constellations and dual-frequency techniques for significant performance improvements. The development and standardization for dual-frequency and multi-constellation SBAS and GBAS are currently ongoing. It is thus expected that with these new techniques a significant performance improvement will be possible compared to the results presented in this paper.

CONCLUSION

In this paper we showed that the use of the GBAS DCPS may provide integrity for UAV users at levels significantly better than what can be achieved with SBAS today. Further performance improvements are possible by reducing the currently standardized k-factor in the GBAS DCPS to bound for the required level of integrity in the foreseen operation. An area of concern currently still unresolved is the impact that anomalous ionospheric behavior can cause. It is suggested that other external information from other GBAS ground stations or external reference stations can be used to resolve this issue. However, the GBAS DCPS concept needs to be further developed in order to provide the necessary integrity assurance for autonomous operations.

ACKNOWLEDGMENTS

The results presented in this paper were developed within a project funded by Swiss FOCA under grant number SFLV2019-038. The authors would like to further thank Natali Cacciopoli and the Pegasus-Team at Eurocontrol for the provision of the Pegasus tool and their kind support in the evaluations!

REFERENCES

1. International Civil Aviation Organization (ICAO), “Annex 10 to the Convention on International Civil Aviation. Aeronautical Telecommunications. Volume I. Radio Navigation Aids.”, July 2018
2. RTCA DO-246E GNSS-Based Precision Approach Local Area Augmentation System (LAAS) Signal-in-Space Interface Control Document (ICD), RTCA, July 2017
3. C. A. Shively and R. Niles, "Safety Concepts for Mitigation of Ionospheric Anomaly Errors in GBAS," in Proc. ION NTM, San Diego, CA, USA, 2008.
4. Kim, M., et al., “GNSS Airborne Multipath Error Modeling Under UAV Platform and Operating Environment”, *Journal of Positioning, Navigation, and Timing*, *March 2015*, vol. 4, no. 1, pp. 1–7
5. Harris, M., Schlais, P., Murphy, T., Joseph, A., Kazmierczak, J. “GPS and GALILEO Airframe Multipath Error Bounding Method and Test Results”, *Proceedings of the 33rd International Technical Meeting of the Satellite Division of The Institute of Navigation (ION GNSS+ 2020) September 21 - 25, 2020,* pp. 114-139
6. Pegasus Software: Available for download at https://www.eurocontrol.int/tool/pegasus (Accessed January 19, 2022)
7. Park, Y. S., Pullen, S., and Enge, P., “Mitigation of Anomalous Ionosphere Threat to Enhance Utility of LAAS Differentially Corrected Positioning Service (DCPS)”, June 2008
8. Murphy, T., Harris, M., “GBAS Differentially Corrected Positioning Service Ionospheric Anomaly Errors Evaluated in an Operational Context”, *Proceedings of the 2010 International Technical Meeting of The Institute of Navigation, San Diego, CA, January 2010*, pp. 394-410.
9. Park, Y. S., Pullen, S., and Enge, P., “Enabling the LAAS Differentially Corrected Positioning Service (DCPS): Design and Requirements Alternatives”, September 2009
10. Caamano, M., Juan, J. M., Felux, M., Gerbeth, D., Gonzalez-Casado, G., & Sanz, J. (2021). Network-based ionospheric gradient monitoring to support GBAS. *NAVIGATION, Journal of the Institute of Navigation*, *68*(1), 135-156.